Eur. Phys. J. B **41**, 495–501 (2004)
DOI: 10.1140/epjb/e2004-00343-2

THE EUROPEAN PHYSICAL JOURNAL B

Modulational instability on triangular dynamical lattices with long-range interactions and dispersion

M. Stepić[1,a], A. Maluckov[2], Lj. Hadžievski[3], F. Chen[1], D. Runde[1], and D. Kip[1]

[1] Institute of Physics and Physical Technologies, Clausthal Technical University, 38678 Clausthal-Zellerfeld, Germany
[2] Faculty of Sciences and Mathematics, University of Niš, 18000 Niš, Serbia and Montenegro
[3] Vinča Institute of Nuclear Sciences, P.O.B. 522, 11001 Belgrade, Serbia and Montenegro

Received 11 May 2004
Published online 5 November 2004 –

Abstract. The influence of long-range interactions on the stability of stationary solutions of triangular lattices described by the continuum-discrete nonlinear Schrödinger equation is analyzed. By virtue of the linear stability analysis and a variational approach we demonstrate that both soliton array and continuous-wave solutions are modulationally unstable. Analytical expressions for instability thresholds and growth rate spectra are presented and compared with the corresponding results in the approximation of a nearest neighbor interaction.

PACS. 42.65.Tg Optical solitons; nonlinear guided waves – 42.81.Dp Propagation, scattering, and losses; solitons

1 Introduction

Modulational instability (MI) represents one of the most basic effects associated with wave propagation in nonlinear media. It consists of the instability of nonlinear plane waves against weak long-scale modulations with frequencies (wave numbers) lower than some critical value. This instability can be regarded as a predecessor for the formation of temporal, spatial, or spatio-temporal patterns. MI, which exist due to an interplay between dispersive/diffraction effects and nonlinearity, is observed and thoroughly studied in various physical systems, such as plasmas [1], fluids [2], nonlinear optics [3–9], and long Josephson junctions [10]. We direct the readers interested in this topic to a comprehensive review paper by Abdullaev et al. [11].

Continuous-discrete systems, such as DNA molecule chains, arrays of coupled Josephson junctions [12], and, especially, nonlinear fiber or waveguide arrays [6–8], have attracted a lot of attention recently. Here, contrary to solely discrete systems, which can be modelled within the framework of the discrete nonlinear Schrödinger equation (DNLS) [13,14], one has to incorporate the effect of dispersion along the lattice elements. These multidimensional systems could be fairly described by virtue of the continuous-discrete nonlinear Schrödinger (CDNLS) equation, which represents a system of linearly coupled nonlinear partial differential equations. If the coupling between the elements is weak enough one can treat this problem within the nearest-neighbor approximation (NNI), see [6,7,12,13], for example. Otherwise, the influence of more lattice elements (sometimes even all of them) must be included leading to a more complicated model with long-range interactions [8,15–17]. With this model one might, for example, depict a vibron energy transport in biopolymers with dipole-dipole interactions [18] and nonlinear localized modes in photonic crystal waveguides [19].

Precisely the rapid progress in fabrication of photonic band-gap crystals [20–22] strengthened the interest in non-square geometries. It was realized that in such crystals, as well as in various chemical systems [23], both honeycomb (hexagonal) and triangular (TA) lattices are pertinent substrate structures. These non-square lattices are investigated in the context of their self trapping dynamics [24], the existence and stability of localized states [25], vortex-vacancy interactions in two-dimensional easy-plane magnets [26], granular matter [27], etc.

The aim of this article is to explore MI of both continuous wave (CW) and soliton array (SA) solutions of a TA lattice within the CDNLS dynamical model with long-range interactions. Up to date, within such systems, MI was studied mainly for the case of the simplest square (SQ) lattice. The paper is organized as follows: we define the basic evolution equation and give the CW and the SA solutions of the model in Section 2. In Section 3 we represent a linear stability analysis based on an energetic principle

[a] e-mail: milutin.stepic@tu-clausthal.de

and a variational approach, which were originally developed for the continuum NLS model [28,29] and recently successfully extended to various continuous-discrete systems with square geometry. Here the explicit analytical expressions for the instability thresholds and the growth rate spectra are given and compared with the analogous results from SQ lattices. The concluding remarks are placed in Section 4.

2 Model

The dynamics of a TA lattice with nonlinearly and nonlocally interacting elements in the anomalous dispersion regime could be adequately described with the following CDNLS model equation

$$i\frac{\partial\psi_{\vec{r}}}{\partial t}+\frac{\partial^2\psi_{\vec{r}}}{\partial z^2}+2\psi_{\vec{r}}|\psi_{\vec{r}}|^2+\sum_{\vec{r'}\ (\vec{r'}\neq\vec{r})}J_{|\vec{r'}-\vec{r}|}(\psi_{\vec{r'}}-\psi_{\vec{r}})=0, \tag{1}$$

where $\vec{r}=(m,n,0)$ is the discrete lattice vector in a $m-n$ plane ($m=0,\pm1,\pm2,...,M;\ n=0,\pm1,\pm2,...,N$), which is presented in Figure 1. The spatial continuous coordinate along the lattice elements is z while $\psi_{\vec{r}}=\psi_{m,n}$ is the wave function of the (m,n)th lattice element. The nonlocal interaction term $J_{|\vec{r'}-\vec{r}|}$ describes a long-range isotropic coupling between lattice elements and depends on the distance between interacting elements. This interaction model is quite general and enables a mathematical modelling of a variety of discrete two-dimensional dispersive physical systems with long-range interactions. The interaction model for a one-dimensional DNLS lattice with a power law dependence on the distance between interacting elements was originally proposed in [15]. In our case, for the CDNLS model equation (1) with an equilateral TA lattice whose inter-element distance is equal to 1, the power law dependence can be written in the form

$$J_{|\vec{r'}-\vec{r}|}=\frac{1}{|\vec{r'}-\vec{r}|^p}. \tag{2}$$

This interaction model may conveniently depict a wide class of different discrete dispersive physical systems with long-range isotropic interactions like propagation of optical pulses in nonlinear fiber arrays, excitation transfer in quasi two-dimensional molecule crystals ($p=3$), and DNA molecule chains with a long-range Coulomb interaction ($p=1$).

Our model equation has a Hamiltonian structure and can be written as $i\partial\psi_{\vec{r}}/\partial t=\delta H/\delta\psi^*_{\vec{r}}$, where H is the Hamiltonian defined by

$$H=\sum_{\vec{r}}\int_{-\infty}^{\infty}\Bigg(\sum_{\vec{r'}(\vec{r'}\neq\vec{r})}J_{\vec{r'}-\vec{r}}(\psi_{\vec{r'}}-\psi_{\vec{r}})\psi^*_{\vec{r}}+|\,(\psi_{\vec{r}})_z\,|^2-|\psi_{\vec{r}}|^4\Bigg)dz. \tag{3}$$

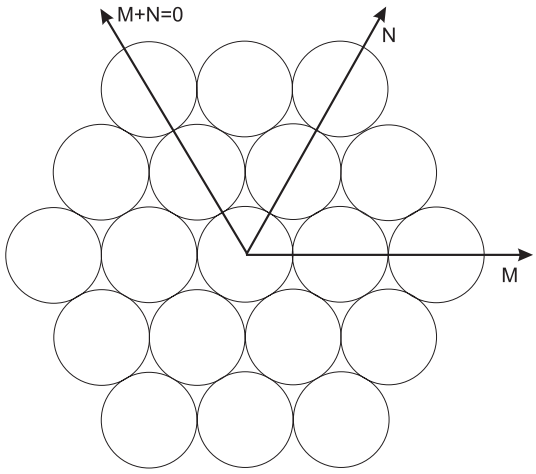

Fig. 1. A coordinate system used for the triangular lattice.

In the above expression for the first conserved quantity of the system the index z denotes the partial derivative with respect to the variable z. Another conserved quantity of equation (1) is the power $P=\sum_{\vec{r}}\int_{-\infty}^{\infty}|\psi_{\vec{r}}|^2dz$.

For the TA lattice with periodic boundary conditions imposed on the discrete dimensions $\vec{r}$ one may consider a set of lattice independent stationary solutions of equation (1) in the form $\psi_{\vec{r}}=f(z)\ e^{i\lambda^2t}$, where λ is a real parameter. We shall restrict our stability study to two particularly simple and most frequently studied stationary solutions. The first one is the uniform CW solution $f_{CW}=\lambda/\sqrt{2}$, while the second one is the SA solution, given by $f_{SA}=\lambda/\cosh(\lambda z)$. In both cases the parameter λ is related to the amplitude of the wave function.

3 Stability analysis

Because MI of the uniform multidimensional CW solution is a forerunner of soliton formation and such optical soliton lattices have a great potential (for example in the field of the self-adjustable waveguides [30]) the investigation of the stability of these stationary solutions is an important task. In order to check their stability properties we have added small, in-phase, square integrable perturbations to the system

$$\psi_{\vec{r}}(x,t)=[f(z)+\delta f_{\vec{r}}(z,t)]e^{i\lambda^2t},\quad |\delta f_{\vec{r}}|\ll|f|. \tag{4}$$

Substituting equation (4) into equation (1) and linearizing with respect to the small perturbations $\delta f_{\vec{r}}$, we get

$$i\frac{\partial\delta f_{\vec{r}}}{\partial t}+\frac{\partial^2\delta f_{\vec{r}}}{\partial z^2}-\lambda^2\delta f_{\vec{r}}+2|f|^2(2\delta f_{\vec{r}}+\delta f^*_{\vec{r}})+\sum_{\vec{r'}\ (\vec{r'}\neq\vec{r})}J_{\vec{r'}-\vec{r}}(\delta f_{\vec{r'}}-\delta f_{\vec{r}})=0. \tag{5}$$

In order to find sufficient conditions for the linear instability we are going to assume perturbations with a simple

harmonic dependence on the discrete dimensions $\vec{r}$ in a form [6,8] $\delta f_{\vec{r}}(z,t) = (a+ib)\cos(k_m m)\cos(k_n n)$, where $k_m = 2\pi/(2M+1)$ and $k_n = 2\pi/(2N+1)$ are discrete wave numbers. It is rather easy to obtain the following eigenvalue problem from the last two equations

$$\frac{\partial b(z,t)}{\partial t} = -\hat{L}_+ a(z,t),$$
$$\frac{\partial a(z,t)}{\partial t} = \hat{L}_- b(z,t), \tag{6}$$

where $\hat{L}_\pm$ are the linear second-order differential operators defined by

$$\hat{L}_+ = -\frac{\partial^2}{\partial z^2} + \lambda^2 - 6f^2(z) + \Sigma(M,N),$$
$$\hat{L}_- = -\frac{\partial^2}{\partial z^2} + \lambda^2 - 2f^2(z) + \Sigma(M,N). \tag{7}$$

The complete discrete properties of the system described by the operators $\hat{L}_\pm$ are taken into account through the interaction term $\Sigma(M,N)$, which is given by the following expression

$$\Sigma(M,N) = 4\Bigg[\sum_{m=1}^{M} J_{m,0}\sin^2(k_m m/2) + \sum_{n=1}^{N} J_{0,n}\sin^2(k_n n/2)\Bigg] - 2\sum_{m=1}^{M} J_{m,-m}[\cos(k_m m)\cos(k_n m) - 1] - 2 \times \sum_{m=1}^{M}\sum_{n=1}^{N} J_{m,n}[\cos(k_m m)\cos(k_n n) - 1], \tag{8}$$

where the whole plane is reduced to the first sextant. This interaction term is always positive and depends both on the lattice dimensions and the form of the interaction between the lattice elements. The first three sums account for long-range interactions along directions which coincide with the symmetry axes of the TA lattice shown in Figure 1, while the last term covers the remaining space.

3.1 Stability of the CW solution

In the case $f_{CW} = \lambda/\sqrt{2}$ the differential operators $\hat{L}_\pm$ are homogeneous and stability analysis is straightforward. The Fourier transform $(e^{-i\omega t + ikz})$ of equations (6) provides the following dispersion relation

$$\omega^2 = \left(k^2 + \Sigma\right)\left(k^2 - 2\lambda^2 + \Sigma\right). \tag{9}$$

Instability occurs for $\omega^2 < 0$, which leads to the following threshold condition

$$\lambda^2 > \frac{k^2}{2} + \frac{\Sigma(M,N)}{2}. \tag{10}$$

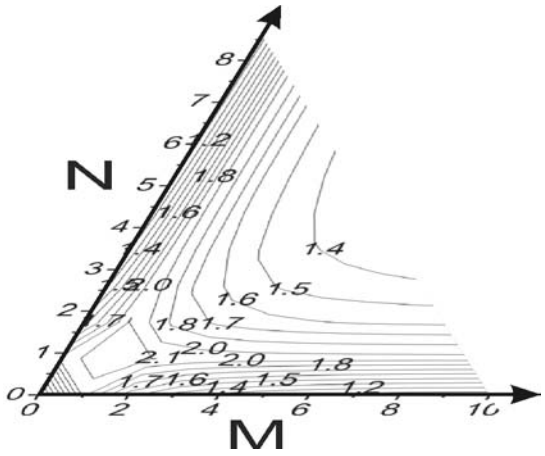

Fig. 2. Instability threshold λ_c as a function of the size of the two-dimensional lattice (M,N) in the nearest-neighbor approximation for $k = \sqrt{2}$.

As can be seen from equation (10), the lowest threshold is for an excitation of small wave-number (long-wavelength) perturbations corresponding to MI.

In the case of the NNI this instability threshold is given by

$$\lambda^2 > \lambda_c^2 = \frac{k^2}{2} + 2\sin^2(k_m/2) + 2\sin^2(k_n/2) - [\cos(k_m)\cos(k_n) - 1]. \tag{11}$$

The dependence of λ_c on the size of the lattice is shown as a contour plot in Figure 2 for the case when $k = \sqrt{2}$. The instability threshold decreases with the enlargement of the lattice and (in the first sextant) it has minima for the direction which coincides with the axis of symmetry of the angle which is determined by m and n axes. Comparing this result with the corresponding one (Eq. (19)) from [8], where a similar problem but for SQ lattices was investigated, it is easy to realize that the instability threshold for the CW solution of TA lattices is always higher than the analogous threshold for SQ lattices. The reason for this is a purely geometric one: as higher is the number of the neighbors in an elementary cell (which is 6 in the TA lattice and 4 in the square one) the stronger is the resistance to changes in the system. In Figure 3, where we present $\Delta\lambda = \lambda_{cTA} - \lambda_{cSQ}$ as a function of the number of the elements of lattices with $M = N$, one can see that the difference between the thresholds for these lattices is biggest when $M = 3$ and that this difference is practically constant for larger lattices.

The corresponding result with long-range interactions between the elements of the TA lattice, where we use the interaction model with a power law dependence of the distance between the interacting elements

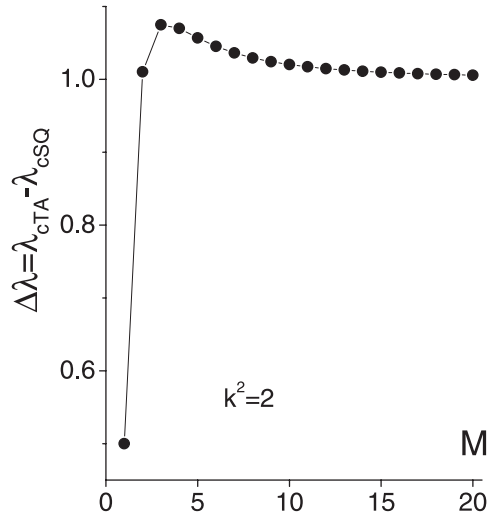

Fig. 3. Value of $\Delta\lambda$ as a function of the size of the lattice with $M = N$ and for $k = \sqrt{2}$ along the most unstable direction.

$J_{m,n} = (m^2 + n^2 + mn)^{-p/2}$, reads

$$\lambda^2 > \frac{k^2}{2} + 2\left[\sum_{m=1}^{M}\frac{\sin^2(k_m m/2)}{m^p} + \sum_{n=1}^{N}\frac{\sin^2(k_n n/2)}{n^p}\right] - \sum_{m=1}^{M}\frac{[\cos(k_m m)\cos(k_n m)-1]}{m^p} - \sum_{m=1}^{M}\sum_{n=1}^{N}\frac{[\cos(k_m m)\cos(k_n n)-1]}{(m^2+n^2+mn)^{\frac{p}{2}}}. \quad (12)$$

This result reveals that, due to the increased inertia of the system, the instability threshold for long-range interactions is higher when compared to the corresponding threshold within the NNI. The instability threshold λ_c for long-range interactions along the most unstable direction in the first sextant as a function of the size of the triangular lattice (with $M = N$) for $k = \sqrt{2}$ and for a few different values of the interaction parameter p is given in Figure 4. The value $p = 3$ corresponds to the case of isotropic dipole-dipole interactions discussed in [18] for the two-dimensional DNLS lattice model. The stabilizing influence of the long-range interaction is obvious.

3.2 Stability of the SA solutions

Stability analysis of the SA solutions becomes more complicated due to an explicit z dependence of the differential operators $\hat{L}_\pm$. However, the fact that the discrete properties of the system are incorporated into the operators $\hat{L}_\pm$ only through the term $\Sigma(M, N)$, enables a direct application of mathematical methods developed for the stability analysis of continuum models. In order to find the instability threshold and to get detailed spectra of the growth rate, we have applied a generalized energetic principle [28] and a variational method [29] to our model. These methods were originally introduced for stability study of continuum NLS equation solutions.

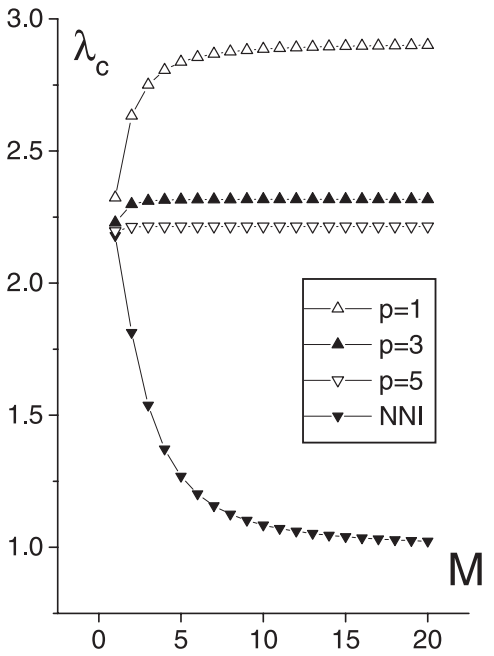

Fig. 4. Instability threshold λ_c along the most unstable direction in the first sextant as a function of the size of the triangular lattice with $M = N$, $k = \sqrt{2}$, and for different values of the parameter p.

Here it is convenient to replace $\lambda z \to z$ and to express the operators $\hat{L}_\pm$ in the form

$$\hat{L}_+ = \lambda^2(\hat{S}_+ + \mu - 5),$$
$$\hat{L}_- = \lambda^2(\hat{S}_- + \mu - 1), \quad (13)$$

where μ is a parameter containing information about the discreteness of the system, defined by

$$\mu = \frac{\Sigma}{\lambda^2}, \quad (14)$$

and $\hat{S}_\pm$ are Sturm-Liouville-type operators

$$\hat{S}_+ = -\frac{\partial^2}{\partial z^2} + 6\tanh^2(z),$$
$$\hat{S}_- = -\frac{\partial^2}{\partial z^2} + 2\tanh^2(z). \quad (15)$$

The spectra of these operators can be found in [31]. The smallest eigenvalues $\sigma_\pm^{(0)}$ and corresponding eigenfunctions $\psi_\pm^{(0)}$ in the discrete part of the spectrum are

$$\sigma_-^{(0)} = 1; \quad \psi_-^{(0)} = 1/\cosh(z),$$
$$\sigma_+^{(0)} = 2; \quad \psi_+^{(0)} = 1/\cosh^2(z). \quad (16)$$

The procedure of the energetic principle, which is described in detail in [29], demands one to find regions of the parameter μ where the operators $\hat{S}_\pm$ are positive definite or indefinite. Since the Sturm-Liouville operators $\hat{S}_\pm$ are positive definite and posses only positive eigenvalues it is

straightforward to find that the operator $\hat{L}_-$ is positive definite for $\mu > 0$, while the operator $\hat{L}_+$ is indefinite for $0 < \mu < 3$ and positive definite for $\mu > 3$. According to the energetic principle sufficient conditions for instability are satisfied in the region $0 < \mu < 3$, where the operator $\hat{L}_+$ is indefinite. On the other hand, the system is stable for $\mu > 3$, where the operators $\hat{L}_\pm$ are positive definite. These results lead to the next instability condition

$$\lambda > \lambda_c = \frac{\sqrt{\Sigma(M,N)}}{\sqrt{3}}. \tag{17}$$

As noticed in [8] this result, for $k = 0$, differs from the corresponding result for the CW solution only in a numerical factor $\sqrt{2/3} \approx 0.8165$. This fact implies that all corresponding explicit results for the instability thresholds for the SA solutions might be derived from the expressions given by equations (10–12) for the instability thresholds of the CW solutions (one has to put $k = 0$ and multiply by the factor 0.8165). Moreover, the form of the curve shown in Figure 2 is the same as in the case of the AS solution.

By virtue of the energy principle it is possible to obtain only a limited part of information, namely, about the instability threshold. In order to calculate the growth rate spectral structure of the instability, one may use a variational approach, originally introduced for the continuum NLS equation in [29] and first generalized to the continuum-discrete 1D NLS equation with NNI in [32]. For the normal exponentially growing modes $a(t,z) = a(z)\exp(\gamma t)$ and $b(t,z) = b(z)\exp(\gamma t)$ with the growth rate γ, the eigenvalue equations (6) are transformed, with the substitution $\lambda z \to z$, into

$$\begin{aligned} \hat{L}_+ a(z) &= -\Gamma b(z), \\ \hat{L}_- b(z) &= \Gamma a(z), \end{aligned} \tag{18}$$

where $\Gamma = \gamma/\lambda^2$ is the normalized growth rate. These equations may be derived from the variation of the action $\delta S = \delta \int_{-\infty}^{\infty} \mathcal{L}(a, a_z, b, b_z, z)dz$, where the Lagrangian $\mathcal{L}$ is given by

$$\mathcal{L} = \frac{1}{2}\left(a_z^2 + b_z^2\right) + \left[\frac{\mu+1}{2} - \frac{3}{\cosh^2(z)}\right] a^2 + \left[-\frac{\mu+1}{2} + \frac{1}{\cosh^2(z)}\right] b^2 + \Gamma ab. \tag{19}$$

The main idea of the variational approach is to define a set of test functions $\tilde{a}(z)$ and $\tilde{b}(z)$ with some variational parameters and to calculate the action integral S. Obviously, with this approach, the obtained results will critically depend on our choice of the test functions. It was shown and also numerically confirmed in [8,29,32] that a good choice for these functions are the eigenfunctions of the operators $\hat{L}_\pm$ for marginally stable states ($\Gamma = 0$)

$$\begin{aligned} a(z) &= 0\ ,\ b(z) = \frac{1}{\cosh(z)}\ , \quad \mu = 0, \\ a(z) &= \frac{1}{\cosh^2(z)}\ ,\ b(z) = 0\ , \quad \mu = 3. \end{aligned} \tag{20}$$

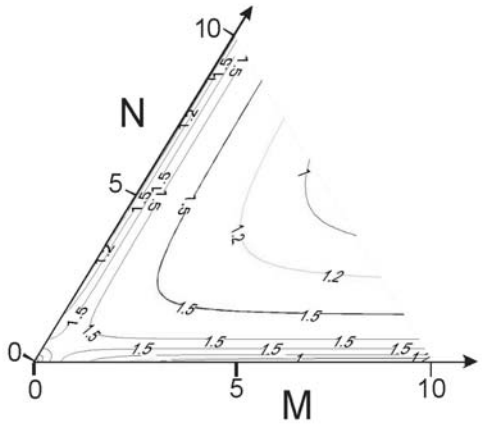

Fig. 5. Normalized growth rate Γ as a function of the size of the triangular lattice in the nearest-neighbor approximation, and for $\lambda = 2$.

Assuming test functions with two variational parameters α and β in the form

$$\tilde{a}(z) = \frac{\alpha}{\cosh^2(z)},\ \ \tilde{b}(z) = \frac{\beta}{\cosh(z)}, \tag{21}$$

we have found the action integral $S = 2\alpha^2(\frac{\mu}{3} - 1) - \mu\beta^2 + \frac{\pi}{2}\Gamma\alpha\beta$. The following expression for the growth rate structure

$$\Gamma(\mu) = \frac{4\sqrt{2}}{\pi\sqrt{3}}\sqrt{\mu(3-\mu)}, \tag{22}$$

is obtained from the conditions $\partial S/\partial\alpha = \partial S/\partial\beta = 0$.

The instability threshold λ_c corresponds to the marginally stable mode $\Gamma = 0$ in the dispersion relation (22). The expression for the threshold calculated from equation (22) coincides, as expected, with the expression (17) obtained by applying the energetic principle.

Replacing the particular expressions for μ into equation (22) for lattices with different types of interactions (nearest-neighbor or long-range) we can readily obtain explicit formulae for the corresponding growth rate structure. So, for the TA lattice with the NNI, we get

$$\begin{aligned} \Gamma = \frac{4\sqrt{2}}{\lambda^2\pi\sqrt{3}}\Big(&4\left[\sin^2(k_m/2) + \sin^2(k_n/2)\right] \\ &-2\left[\cos(k_m)\cos(k_n) - 1\right]\Big)^{1/2} \\ &\times\Big(3\lambda^2 - \{4\big[\sin^2(k_m/2) \\ &+\sin^2(k_n/2)\big] - 2\left[\cos(k_m)\cos(k_n) - 1\right]\}\Big)^{1/2}. \end{aligned} \tag{23}$$

We present the dependence of Γ on the size of the lattice as a contour plot in Figure 5 for $\lambda = 2$.

In the case of long-range interactions, where the interaction model with a power law dependence on

the distance between the interacting elements $J_{m,n} = (m^2+n^2+mn)^{-p/2}$ is applied, one can obtain

$$\Gamma = \frac{4\sqrt{2}}{\lambda^2\pi\sqrt{3}} \left\{ 4\left[\sum_{m=1}^{M} \frac{\sin^2(k_m m/2)}{m^p} + \sum_{n=1}^{N} \frac{\sin^2(k_n n/2)}{n^p}\right] - 2\sum_{m=1}^{M} \frac{[\cos(k_m m)\cos(k_n m)-1]}{m^p} - 2\sum_{m=1}^{M}\sum_{n=1}^{N} \frac{[\cos(k_m m)\cos(k_n n)-1]}{(m^2+n^2+mn)^{\frac{p}{2}}} \right\}^{1/2} \times \left\{ 3\lambda^2 - 4\left[\sum_{m=1}^{M} \frac{\sin^2(k_m/m2)}{m^p} + \sum_{n=1}^{N} \frac{\sin^2(k_n n/2)}{n^p}\right] + 2\sum_{m=1}^{M} \frac{[\cos(k_m m)\cos(k_n m)-1]}{m^p} + 2\sum_{m=1}^{M}\sum_{n=1}^{N} \frac{[\cos(k_m m)\cos(k_n n)-1]}{(m^2+n^2+mn)^{\frac{p}{2}}} \right\}^{1/2}. \quad (24)$$

We monitor, for the sake of simplicity, the behavior of this growth rate only along the most unstable direction of the lattice with $M = N$, i.e., along the diagonal of the first sextant. In Figure 6, where $\lambda = 2$, one might see how the normalized growth rate Γ depends on the size of the lattice for various values of the interaction parameter p. The result in the NNI approximation practically corresponds to the result of the power law interaction for $p = 5$. Moreover, it is clear that the influence of long-range interactions is more pronounced for larger lattices. Figure 7 depicts the dependence of Γ on the soliton parameter λ for a lattice with $M = N = 4$ and for different values of the parameter p. It is easy to notice how an increase of the radius of the interaction influences the growth of the threshold amplitude for the onset of the instability. For higher values of the parameter λ where, independently of the values of the parameter p, the condition for the onset of the instability is fulfilled, one might notice that the chosen exponential perturbation spreads the fastest for $p = 1$.

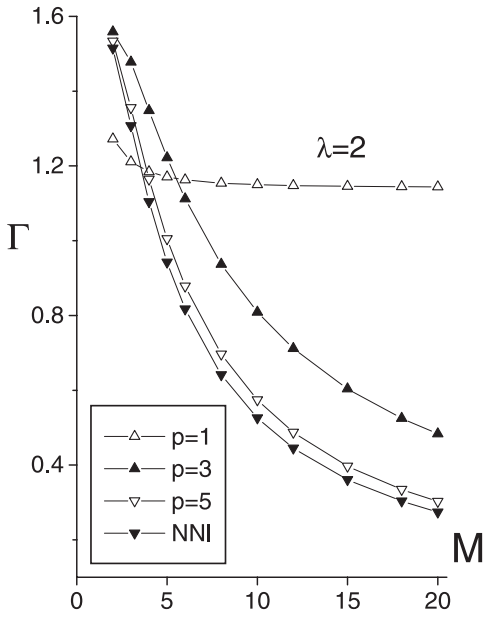

Fig. 6. Normalized growth rate Γ as a function of the size of the triangular lattice for different values of the parameter p and $\lambda = 2$.

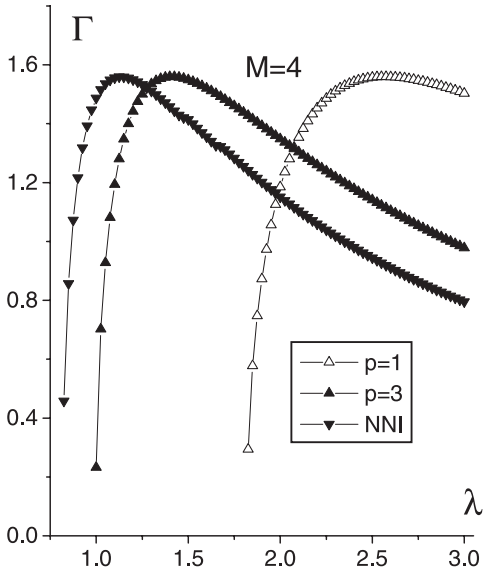

Fig. 7. Normalized growth rate Γ as a function of the soliton parameter λ for lattice with $M = N = 4$ and for various values of the parameter p.

4 Conclusion

To conclude, an attempt to examine the problem of modulational instability of stationary solutions on a triangular lattice is presented. In media with cubic nonlinearity and dispersion the continuous-discrete nonlinear Schrödinger (CDNLS) equation can be considered as an adequate prototype equation. We paid attention to continuous-discrete nonlinear systems with long-range interactions between the elements, such as photonic crystals, nonlinear fiber arrays, and DNA molecule chains. Usage of a standard linear stability analysis revealed that the first, continuous wave, stationary solution is unstable with respect to small in-phase perturbations. The linear stability of the second, soliton array, stationary solution is solved by virtue of an energetic principle and a variational method, which were originally developed for the continuum nonlinear Schrödinger equation [28,29]. We have calculated explicit expressions for the instability thresholds and growth rate spectra valid for the CDNLS on a triangular lattice with long-range isotropic coupling between the elements of the lattice. Furthermore, we obtained explicit formulae for long-range isotropic interactions with a power law dependence on the distance between the interacting elements. Our results are compared with the corresponding results from square lattices. The stationary solutions of the triangular lattice have higher instability thresholds than for the square lattice. The stabilizing role of the long-range

interaction on the stability of both stationary solutions is confirmed and it was shown that, when the conditions for the onset of the instability are fulfilled, the growth rate of the perturbation is proportional to the radius of the long-range interaction. Our results may be interesting not only for the area of nonlinear optics but also in biology, chemistry, and condensed matter physics [33].

This work is carried out under the auspices of the German Federal Ministry of Education and Research (BMBF, grant DIP-E6.1), INTAS (contract 01-0481), and by the Ministry of Science, Development and Technologies of Republic Serbia, Project 1964. F. Chen gratefully acknowledges financial support of the Alexander von Humboldt Foundation.

References

1. A. Hasegawa, Phys. Fluids **15**, 870 (1972)
2. T.B. Benjamin, J.E. Feir, J. Fluid Mech. **27**, 417 (1967)
3. G.A. Askar'yan, Zh. Eksp. Teor. Fiz. **42**, 1567 (1962)
4. K. Tai, A. Hasegawa, A. Tomita, Phys. Rev. Lett. **56**, 135 (1986)
5. M.D. Iturbe-Castillo et al., Opt. Lett. **20**, 1853 (1995)
6. A.B. Aceves et al., Phys. Rev. Lett. **75**, 73 (1995)
7. S. Darmanyan, I. Relke, F. Lederer, Phys. Rev. E **55**, 7662 (1997)
8. Lj. Hadžievski, M. Stepić, M.M. Škorić, Phys. Rev. B **68**, 014305 (2003)
9. D. Kip et al., Science **290**, 495 (2000)
10. F.Kh. Abdullaev, Tech. Phys. Lett. **23**, 52 (1997)
11. F.Kh. Abdullaev, S.A. Darmanyan, J. Garnier, Progress in Optics **44**, 303 (2002)
12. L.M. Floría et al., Europhys. Lett. **36**, 539 (1996)
13. Yu.S. Kivshar, M. Peyrard, Phys. Rev. A **46**, 3198 (1992)
14. E.W. Laedke et al., JETP Lett. **62**, 677 (1995)
15. Yu.B. Gaididei et al., Phys. Rev. E **55**, 6141 (1997)
16. P.L. Christiansen et al., Eur. Phys. J. B **19**, 545 (2001)
17. P.G. Kevrekidis et al., Phys. Rev. E **64**, 066606 (2001)
18. P.L. Christiansen et al., Phys. Rev. B **57**, 11303 (1998)
19. S.F. Mingaleev, Yu.S. Kivshar, R.A. Sammut, Phys. Rev. E **62**, 5777 (2000)
20. J.C. Knight et al., Opt. Lett. **21**, 1547 (1996)
21. Se-Heon Kim et al., Appl. Phys. Lett. **81**, 2499 (2002)
22. M.A. Kaliteevski et al., J. Phys.: Condens. Matter **15**, 785 (2003)
23. R. Atencio et al., New J. Chem. **23**, 461 (1999)
24. M.I. Molina, Mod. Phys. Lett. B **13**, 837 (1999)
25. P.G. Kevrekidis, B.A. Malomed, Yu.B. Gaididei, Phys. Rev. E **66**, 016609 (2002)
26. G.M. Wysin, Phys. Rev. B **68**, 184411 (2003)
27. G. Oron, H.J. Herrmann, Phys. Rev. E **58**, 2079 (1998)
28. E.W. Laedke, K.H. Spatschek, Phys. Rev. Lett. **41**, 1798 (1978)
29. K. Rypdal, J.J. Rasmussen, Phys. Scr. **40**, 192 (1989)
30. M. Petrović et al., Phys. Rev. E **68**, 055601(R) (2003)
31. P.M. Morse, H. Feshback, *Methods of Theoretical Physics*, Chaps. 6 and 12 (McGraw-Hill, New York, 1953)
32. M. Stepić, Lj. Hadžievski, M.M. Škorić, Phys. Rev. E **65**, 026604 (2002)
33. J.L. Marin, J.C. Eilbeck, F.M. Russel, Phys. Lett. A **248**, 225 (1998); J.L. Marin, J.C. Eilbeck, F.M. Russel in *Nonlinear Science at the Dawn of the 21th Century*, edited by P.L. Christiansen, M.P. Soerensen (Springer, Berlin, 2000), p. 293